# Phenalenone-type phytoalexins mediate resistance of banana plants (*Musa* spp.) to the burrowing nematode *Radopholus similis*

Dirk Hölscher[a,b,1,2], Suganthagunthalam Dhakshinamoorthy[c,1], Theodore Alexandrov[d,e,f,g], Michael Becker[h], Tom Bretschneider[i], Andreas Buerkert[b], Anna C. Crecelius[j], Dirk De Waele[c,k], Annemie Elsen[l], David G. Heckel[m], Heike Heklau[n], Christian Hertweck[i], Marco Kai[o], Katrin Knop[j], Christoph Krafft[p], Ravi K. Maddula[o], Christian Matthäus[p], Jürgen Popp[p,q], Bernd Schneider[a], Ulrich S. Schubert[j,r], Richard A. Sikora[s], Aleš Svatoš[o], and Rony L. Swennen[c,t,u]

[a]Nuclear Magnetic Resonance Research Group, [o]Mass Spectrometry Research Group, [m]Department of Entomology, Max Planck Institute for Chemical Ecology, 07745 Jena, Germany; [b]Department of Organic Plant Production and Agroecosystems Research in the Tropics and Subtropics, University of Kassel, 37213 Witzenhausen, Germany; [c]Laboratory of Tropical Crop Improvement, Division of Crop Biotechnics, Faculty of Bioscience Engineering, Department of Biosystems, University of Leuven, 3001 Leuven, Belgium; [d]Center for Industrial Mathematics, Department of Mathematics, University of Bremen, 28359 Bremen, Germany; [e]Steinbeis Innovation Center for Scientific Computing in Life Sciences, 28359 Bremen, Germany; [f]Scientific Computing in Life Sciences (SCiLS) GmbH, 28359 Bremen, Germany; [g]Skaggs School of Pharmacy and Pharmaceutical Science, University of California, San Diego, La Jolla, CA 92093; [h]Department of Applications Matrix-Assisted Laser Desorption/Ionization - Time of Flight (MALDI-TOF), Bruker Daltonik GmbH, 28359 Bremen, Germany; [i]Department of Biomolecular Chemistry, Leibniz Institute for Natural Product Research and Infection Biology, 07745 Jena, Germany; [j]Laboratory of Organic and Macromolecular Chemistry, Jena Center for Soft Matter, [q]Institute for Physical Chemistry and Abbe Center of Photonics, Department of Chemistry and Earth Sciences, Friedrich Schiller University of Jena, 07743 Jena, Germany; [k]Unit of Environmental Sciences and Management, Department of Nematology, North-West University, Potchefstroom 2520, South Africa; [l]Department of Research and Development, Soil Service of Belgium, 3001 Leuven Heverlee, Belgium; [n]Department of Geobotany, Martin Luther University of Halle-Wittenberg, 06108 Halle, Germany; [p]Workgroup Spectroscopy/Imaging, Institute of Photonic Technology, 07745 Jena, Germany; [r]Dutch Polymer Institute, 5612 AB, Eindhoven, The Netherlands; [s]Institute of Crop Science and Resource Conservation-Phytomedicine, Rheinische Friedrich-Wilhelms-Universität Bonn, 53115 Bonn, Germany; [t]Bioversity International, 3001 Leuven, Belgium; and [u]International Institute of Tropical Agriculture, Croydon CR9 3EE, United Kingdom

Edited by Jerrold Meinwald, Cornell University, Ithaca, NY, and approved November 14, 2013 (received for review August 8, 2013)

**The global yield of bananas—one of the most important food crops—is severely hampered by parasites, such as nematodes, which cause yield losses up to 75%. Plant–nematode interactions of two banana cultivars differing in susceptibility to *Radopholus similis* were investigated by combining the conventional and spatially resolved analytical techniques $^1$H NMR spectroscopy, matrix-free UV-laser desorption/ionization mass spectrometric imaging, and Raman microspectroscopy. This innovative combination of analytical techniques was applied to isolate, identify, and locate the banana-specific type of phytoalexins, phenylphenalenones, in the *R. similis*-caused lesions of the plants. The striking antinematode activity of the phenylphenalenone anigorufone, its ingestion by the nematode, and its subsequent localization in lipid droplets within the nematode is reported. The importance of varying local concentrations of these specialized metabolites in infected plant tissues, their involvement in the plant's defense system, and derived strategies for improving banana resistance are highlighted.**

plant protection | induced plant defense | matrix-free LDI-MSI

Bananas and plantains (*Musa* spp.) are among the world's most important food and cash crops, with a global production of about 138 million tons in 2010. These crops are part of a well-balanced human diet and are a major food staple for more than 400 million people in the tropics (1, 2). About 82% of the world's banana production is consumed locally, particularly in India, China, and many African countries (Table S1) (1, 2). Export of bananas to the northern hemisphere represents an important source of employment in countries such as Costa Rica, Ecuador, Colombia, and the Philippines (Table S2) (1, 2). Banana yields are severely hampered by fungi, insects, and plant-parasitic nematodes. The burrowing nematode, *Radopholus similis* (Cobb, 1893) Thorne, 1949, is the key nematode pathogen, causing yield losses up to 75% (3). *R. similis* is found in all major banana-producing regions of the world; its best-known hosts are bananas, black pepper, *Citrus* spp. (4), and coffee (5). *R. similis* causes extensive root lesions that can lead to toppling of banana plants (6).

Plant-parasitic nematodes have been effectively managed through the use of nematicides. However, their high toxicity has adverse effects on humans and their toxic residues are known to accumulate through nontarget organisms in the food chain (7). After the withdrawal of many effective nematicides, such as methyl bromide, from the market (8), organophosphate and carbamate nematicides are still intensively applied to banana and therefore continue to threaten the health of agricultural workers and the environment (9). Although several biological control approaches, including the application of both single and multiple control organisms—such as *Fusarium oxysporum*, *Paecilomyces lilacinus*, *Trichoderma atroviride* isolates, and *Bacillus firmus*—have proved promising under greenhouse conditions, the control they confer to banana plants most probably does not protect plants for more than one cycle in the field, and most of these organisms have yet to be tested under field conditions (10).

## Significance

The ongoing decline of banana yields caused by pathogens and the use of toxic chemicals to manage them has attracted considerable attention because of the importance of bananas as a major staple food for more than 400 million people. We demonstrate that secondary metabolites (phenylphenalenones) of *Musa* are the reason for differences in cultivar resistance, and detected the phenylphenalenone anigorufone in greater concentrations in lesions in roots of a nematode-resistant cultivar than in those of a susceptible one. An in vitro bioassay identified anigorufone as the most active nematostatic and nematocidal compound. We discovered that large lipid–anigorufone complex droplets are formed in the bodies of *Radopholus similis* exposed to anigorufone, resulting in the nematode being killed.

Author contributions: D.H., S.D., A.B., D.G.H., B.S., R.A.S., and R.L.S. designed research; D.H., S.D., M.B., T.B., A.C.C., H.H., M.K., K.K., R.K.M., and C.M. performed research; D.H., S.D., T.A., T.B., A.C.C., D.D.W., A.E., M.K., K.K., C.K., C.M., J.P., U.S.S., and A.S. analyzed data; and D.H., S.D., T.A., T.B., A.C.C., D.D.W., A.E., C.H., M.K., K.K., C.K., C.M., J.P., B.S., U.S.S., R.A.S., A.S., and R.L.S. wrote the paper.

The authors declare no conflict of interest.

This article is a PNAS Direct Submission.

[1]D.H. and S.D. contributed equally to this work.

[2]To whom correspondence should be addressed. E-mail: hoelscher@ice.mpg.de.

This article contains supporting information online at www.pnas.org/lookup/suppl/doi:10.1073/pnas.1314168110/-/DCSupplemental.

The in-depth investigation of the plant–nematode interactions at the cellular and molecular level could lead to the development of more rational and efficient control strategies (11). The production of toxic, herbivore-deterrent or -repellent secondary metabolites, which is typical for many plant defense systems, is particularly interesting in this context. *Musa* cultivars resistant to *R. similis* have been identified, especially the cultivar Yangambi km5 (Ykm5) (12). Histochemical and ultrastructural investigations of lesions caused by *R. similis* in Ykm5 revealed the accumulation of phenolic compounds in response to infection (13). Unfortunately, many of these studies were based solely on histochemical staining methods and did not identify the chemical structures of nematicidal secondary metabolites (7, 14, 15). Initial phytochemical analyses of *R. similis*-infected roots of the *Musa* cultivar Pisang sipulu identified the phenylphenalenone anigorufone (**1**) as a phytoalexin produced in response to nematode damage and confirmed earlier suggestions of the significant role of phytoalexins in the plant defense system (16). Phenylphenalenones are a group of special phenylpropanoid-derived natural products (17), which are known as Musaceae phytoalexins (18). The activity of phenylalanine ammonia lyase (EC 4.3.15), the entry-point enzyme of the phenylpropanoid pathway, is correlated to the biosynthesis of specific phenylpropanoids involved in defense and was substantially induced in nematode infected roots of Ykm5 (19). Phenylphenalenone-related compounds show biological activity against bacteria, fungi, algae, and diatoms (18, 20–22). The formation of these compounds has been elicited in banana leaves by *Mycosphaerella fijiensis* (Black Sigatoka leaf streak disease), in the fruit peels by *Colletotrichum musae* (anthracnose disease), and in roots and rhizomes by *F. oxysporum* f. sp. *cubense* (Panama disease) and *R. similis* (16, 18, 21, 23).

## Results

**Root Damage and Root Lesions.** In the greenhouse, potted Grande Naine (GN) and Ykm5 plants were inoculated with *R. similis*. Roots of 20-wk-old plants were monitored for nematode damage 12 wk after infection. Root damage was more severe in GN than in Ykm5. Visual observation of infected GN roots revealed large, continuous, and tunnel-like lesions (Fig. 1 *A* and *B*). Moreover, root damage extended to the root bases near the GN corms (Fig. 1*C*). Newly formed root lesions were light red in color. Older lesions were dark red-brownish. In Ykm5, no corm infection was observed and both newly formed and older root lesions were small, discontinuous, dark red-brown in color, and nonexpanding (Fig. 1 *D* and *E*). Uninfected roots of Ykm5 and GN, used as controls, showed no lesions and appeared healthy upon visual inspection.

**Isolation and Identification of Metabolites.** *R. similis* lesions from GN and Ykm5 roots were manually dissected from infected roots under the microscope, and metabolites were extracted from lesion material using ethanol. The intensely red-colored lesions were easily visually distinguishable from healthy, beige-colored root tissues. Equal amounts of roots from uninfected plants were used as controls. Liquid-liquid separation from all of the above four samples resulted in $CHCl_3$, ethyl acetate, 1-butanol, and aqueous subfractions. Preliminary $^1H$ NMR analysis of subfractions of the *R. similis*-infected GN and Ykm5 root material revealed signals in the aromatic range of the spectrum of the $CHCl_3$ extract, whereas the other subfractions did not show aromatic signals of notable intensity. The $CHCl_3$ subfractions were further analyzed for the occurrence of phenylphenalenones. In a first step, the $CHCl_3$ subfractions of all of the samples were purified by semipreparative HPLC. The individually collected fractions were subjected to $^1H$ NMR spectroscopy for identification and the structures of all compounds were identified as typical metabolites and major phytoalexins of *Musa* species (Fig. S1) (18, 21, 23). The phytochemical profiles and the number of secondary metabolites in GN and Ykm5 (Fig. S1) were slightly different. Anigorufone (**1**), hydroxyanigorufone (**2**), irenolone (**5**), 4-phenyl-*1H,3H*-benzo[*de*]isochromene-1,3-dione (**7**), and 4-(4-hydroxyphenyl)-*1H,3H*-benzo[*de*]isochromene-1,3-dione (**8**) were detectable in the extracts of lesions from both cultivars. (2*S*,3*R*)-2,3-Dihydro-2,3-dihydroxy-9-phenylphenalen-1-one (**3**), isoanigorufone (**4**), and anigorootin (**9**) were exclusively found in Ykm5, and methylirenolone (**6**) only in GN. Twice as much anigorufone (**1**), the major specialized metabolite of lesions in both cultivars, was found in Ykm5 compared with GN. Additionally, all minor compounds were present in smaller amounts per kilogram of root material in GN compared with Ykm5. The amounts of the isolated compounds are shown in Table S3.

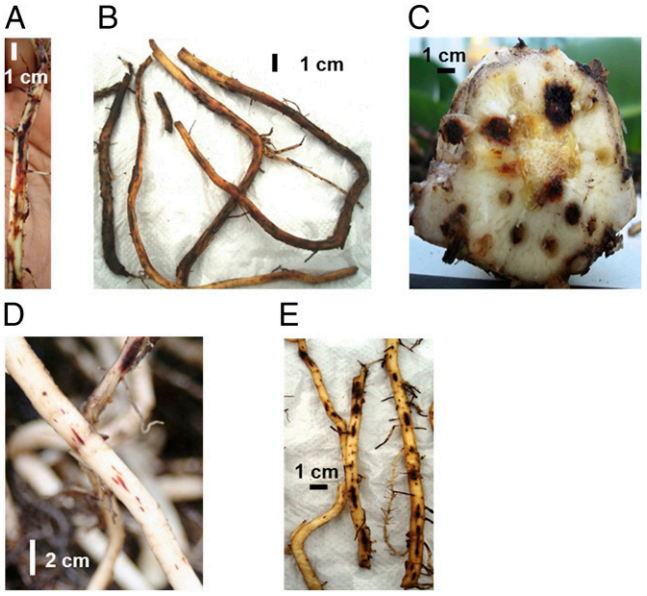


**Fig. 1.** Photographs of the root system of *Musa* spp. cv. GN and *cv.* Ykm5 infected with *R. similis*. (*A*) Young, developing, reddish brown lesions on GN roots. (*B*) Well-developed, tunnel-like, dark brown, older lesions on GN roots. (*C*) Lesions on the root bases of the GN corm. (*D*) Young, developing, reddish-brown lesions on Ykm5 roots. (*E*) Older, small, discontinuous, dark brown lesions on Ykm5 roots.

**Analysis and Interpretation of Laser Desorption/Ionization Mass Spectrometric Imaging Data.** The suitability of matrix-free UV-laser desorption/ionization mass spectrometric imaging (LDI-MSI) to identify secondary metabolites of *Arabidopsis thaliana* and *Hypericum* species (24) encouraged us to use this spatially resolved bioanalytical technique to study the presence of phenylphenalenones in the lesions of GN and Ykm5. The Ultraflex III- and the ultrafleXtreme mass spectrometers allowed the application of a high lateral resolution of 10 μm, enabling the localization of phenylphenalenones in the lesion area (100–200 $\mu m^2$).

The accumulation of secondary metabolites in the lesions was detected by LDI-MSI. The LDI-MSI data obtained from the lesion and the surrounding tissues (Fig. 2) show mass signals of phenylphenalenones precisely at the site of nematode infection. The LDI-MSI images were plotted in SCiLS Lab software (SCiLS) after spectra baseline correction, hotspot removal (by suppressing 1% of most intense pixels), and edge-preserving image-denoising to reduce the pixel-to-pixel variation (25). Within the lesions, *m/z* values of the discovered secondary metabolites (compounds **1**–**9**) were detected, which are consistent with compounds resulting from the phytochemical investigations of the dissected lesions. The *m/z* value of 271 detected within the lesions was assigned to $[M\text{-}H]^+$ of the compounds anigorufone (**1**), **4**, or both (Fig. 2*C*). A signal for compound **7** (*m/z* 273) was found in this area (Fig. 2*D*),

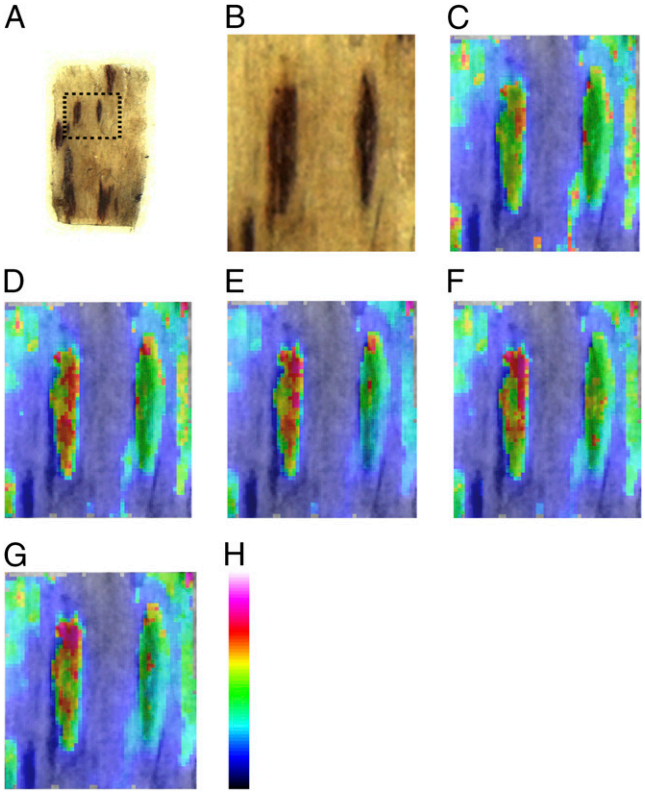


**Fig. 2.** Negative ion mode LDI-MSI of the lesions of Ykm5. (*A*) Optical image of the lesions on Ykm5 roots. (*B*) The region of the lesions subjected to LDI-MSI. The molecular image of section *B* for the *m/z* (*C*) 271, (*D*) 273, (*E*) 287, (*F*) 289, and (*G*) 301. (*H*) False color scale bar.

as well as signals of compound **2** and its 4-phenyl analog **5** (*m/z* 287) (Fig. 2*E*). The signal *m/z* 289 was attributable to the secondary metabolites **3**, **8**, or both (Fig. 2*F*). A signal for the *O*-methyl phenylphenalenone (**6**) of *m/z* 301 was also detectable (Fig. 2*G*). Furthermore, using the ultrafleXtreme, we were able to detect a signal for the dimer **9** at *m/z* 573.

The areas of the lesions were strikingly different from the healthy, uninfected surrounding regions with regard to the presence of secondary metabolites, both in the isolation experiments and in the LDI-MSI investigations. Nevertheless, an elevated ion signal background in single LDI measurements caused by high laser intensities was observed within the uninfected regions of the tissue. As the color mapping indicates only the signal intensity at specific raster points and not the occurrence of a certain compound, color signals appear where only background is detected (Fig. S2).

**Effect of Phenylphenalenones in *R. similis* Motility Bioassay.** To test for antinematode properties of the phenylphenalenone-type phytoalexins, an in vitro bioassay on the motility of *R. similis* was performed with 13 selected phenylphenalenones and related compounds (Fig. S1 and Table S4). The percentage of nematode motility inhibition (nematostatic effect) was monitored after 24, 48, and 72 h of exposure to the compounds.

At both tested concentrations (50 and 100 ppm), anigorufone (**1**), and compounds **2** and **13** showed a nematostatic effect as of 24 h of incubation. This effect was either constant (compound **13**) or increased over time up to 72 h (**1** and **2**). Anigorufone (**1**) showed the strongest activity, with 89% of the nematodes becoming immotile after 72 h of incubation. Similar nematostatic effects were observed for compounds **2**, **4**, **8**, and 4-hydroxy-2-methoxy-9-phenylphenalenone (**11**) at a concentration of 100 ppm. Exposure to 50 ppm resulted in higher percentages of immotile nematodes of 48 h of exposure, in comparison with the 1% ethanol control. The compounds **5**, **9**, methoxyanigorufone (**10**), musanolone C (**12**), and perinaphthenone (**15**) revealed inconsistent nematostatic effects. Methylirenolone (**6**) and dihydroxyanigorootin (**14**) did not show any substantial inhibition of nematode motility (not included in Table S4). The solvent (1% ethanol) exhibited a negligible effect on nematode motility comparable to sterile distilled water.

**Dosage Effect of Anigorufone (1) on *R. similis* Motility Bioassay.** Among the phenalenones tested in the *R. similis* motility bioassay, anigorufone (**1**) was the most active compound at a concentration of 100 ppm (Table S4). Therefore, anigorufone (**1**) was selected for a more detailed investigation of its nematostatic potential. The data obtained at 10, 20, 40, 50, and 100 ppm clearly showed a concentration-dependent effect of anigorufone (**1**) on nematode motility (Fig. S3). At an incubation time of 24 h, the percentage of immotile versus the total number of nematodes increased from nonsignificant 26%, at a concentration of 10 ppm, to significant 50.2% at 40 ppm and 74.3% at 100 ppm. Hence, significantly ($P < 0.05$) higher levels of nematostatic effects were observed from 40 ppm upwards compared with the control (1% ethanol). Increasing the concentration to 150 ppm resulted in partial precipitation of anigorufone (**1**). Compared with the values obtained after 24 h, the motility of nematodes further decreased at incubation times of 48 and 72 h (Fig. S3). The concentration of anigorufone (**1**), which inhibited the motility of 50% of the nematodes ($IC_{50}$) in the bioassay, was 59 μg/mL for an incubation time of 24 h. For an exposure time of 48 h, $IC_{50}$ was 38 μg/mL, and only 23 μg/mL for 72 h of exposure.

**Nematode Ingestion of Anigorufone (1) and Its Detection by LDI-MSI.** A surprising observation was made during the evaluation of the *R. similis* motility bioassay with anigorufone (**1**). Under bright field microscopy (BF), yellow droplets were seen in parts of the bodies of nematodes exposed to high concentrations of anigorufone (**1**) (Fig. 3). These droplets were readily visible because of the natural transparency of the nematode cuticle. Nematodes containing such yellow droplets were subjected to LDI-MSI to identify the yellow pigment. The drying of the nematodes on the indium tin oxide (ITO)-coated conductive glass slides and the high-field vacuum conditions of the LDI-MSI process preserved the position of the nematodes on the slides and allowed pointing the laser precisely at the target region. This aspect was important because the shape of the yellow droplets changed during the drying on the glass slides and during the LDI-MSI measuring process, because the droplets converged. LDI-MSI spectra recorded from yellow regions of *R. similis* nematodes showed an ion peak of *m/z* 273 $[M+H]^+$, corresponding to the molecular mass of anigorufone (**1**) (Fig. 4). LDI-MSI spectra of control nematodes not exposed to anigorufone (**1**) did not show such a signal. Ingestions of large enough amounts of anigorufone (**1**) to be visible by BF always led to nematode mortality. Thus, it has become obvious that anigorufone (**1**) is not only a nematostatic but also a nematocidal compound.

**Raman Microspectroscopy.** Studies were conducted to analyze the chemical composition of the yellow droplets appearing in the bodies of *R. similis* after ingestion of anigorufone (**1**). Recent developments in combining Raman spectroscopy with optical microscopy provided a new noninvasive technique to assess and image biological samples and processes. The technique has recently been successfully applied to identify and visualize lipid droplets in nematodes (26). Fig. 5*A* shows a BF image of part of a *R. similis* nematode using a 60×/NA = 1 water-immersion objective. The Raman image, reconstructed from the integrated areas of the scattering intensities originating from C-H stretching

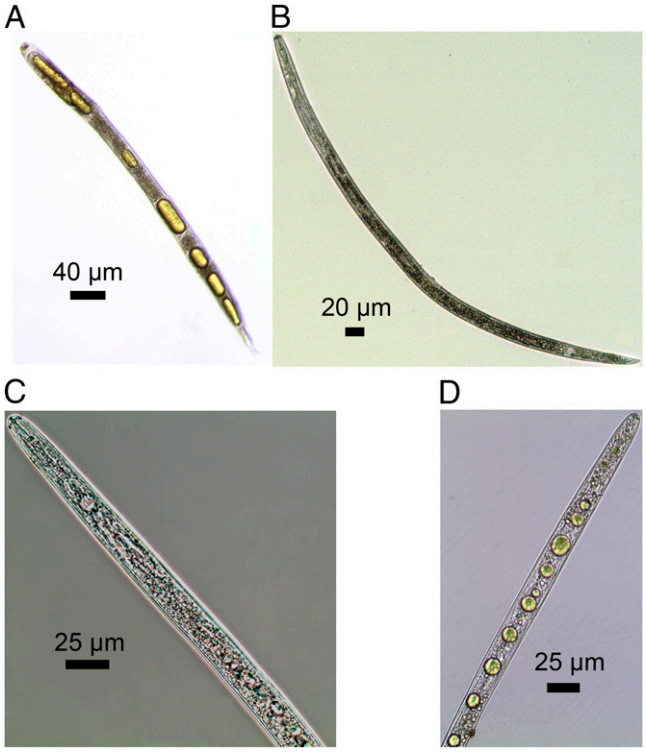


**Fig. 3.** BF microscopic images of *R. similis* from bioassay with anigorufone (**1**) (*A* and *C*) and from negative control, 1% ethanol (*B* and *D*). Nematodes were temporarily fixed for imaging purpose. (*A*) Dead *R. similis* from bioassay with anigorufone (**1**); note yellow droplets in body. (*B*) Adult female *R. similis* after 72 h incubation in control. (*C*) Accumulation of anigorufone (**1**) in small oil droplets throughout the body of a juvenile *R. similis* nematode. (*D*) Anterior body of a *R. similis* showing normal digestive tract.

vibrations of organic molecules of part of the image in Fig. 5*A*, is shown in Fig. 5*B*. Fig. 5*C* was generated from Fig. 5*B* using a spectral decomposition algorithm that searches for the greatest spectral contrast within a given dataset. Subsequently the abundances of the spectral information were plotted. The distribution of lipids is shown in red in Fig. 5*C*, the protein distribution in light blue. Apparently, the lipids are arranged in rather large fat droplets, whereas the abundance of the proteins reveals the internal organization of the organism. Fig. 5*D* shows the associated spectral information. The spectrum shown in light blue exhibits all characteristic features associated with proteins. For example, the scattering intensities between 2,800 and 3,100 $cm^{-1}$ originate from C-H stretching vibrations of the protein residues; the band centered around 1,650 $cm^{-1}$ is a result of stretching motions of the C = O bonds of the peptide backbones; and $CH_2$ scissoring motions can be observed at 1,450 $cm^{-1}$. The red spectrum resembles a typical spectrum of lipids. The intensities of C-H stretching bands between 2,800 and 3,100 $cm^{-1}$ and C-H deformation bands near 1,300 and 1,440 $cm^{-1}$ are more intense than in proteins. Further bands are assigned to C = O bonds of ester groups at 1,740 $cm^{-1}$, C = C groups of unsaturated fatty acid chains at 1,260 and 1,660 $cm^{-1}$, and C-C groups at 1,070 $cm^{-1}$.

## Discussion

Banana cultivars show different grades of susceptibility to the burrowing nematode *R. similis*. The cultivar Grande Naine (GN), which is extensively cultivated for banana fruit production, is susceptible to *R. similis* and, in contrast, the cultivar Yangambi km5 (Ykm5), is largely resistant. The objective of this study was to investigate if secondary metabolites of the *Musa* plant could be the reason for these differences in plant–nematode interaction.

This study provides evidence for the local induction of phenylphenalenone-type secondary metabolites in response to *R. similis* infection in *Musa* spp. LDI-MSI was used with phenylphenalenones and nine phenylphenalenone-type compounds were detected in nematode-induced lesions. These compounds were elucidated by NMR analyses and identified as typical metabolites and major phytoalexins of *Musa* species (21). Anigorufone (**1**) was the most abundant phenylphenalenone-type secondary metabolite present in the nematode-induced lesions of the resistant cultivar Ykm5, as well as in the susceptible cultivar GN. As recently reported for secondary metabolites of *A. thaliana* and *Hypericum* species, LDI-MSI is an effective technique of localizing secondary metabolites in plant tissues (24). Here this technique revealed that the location of phenylphenalenones in *Musa* roots is restricted to the lesions created by *R. similis*.

A significant difference between the two *Musa* cultivars was observed when the mass fraction of the compounds in the lesions was determined. A greater concentration of anigorufone (**1**) and other antinematode phenylphenalenones was discovered in the small lesions in Ykm5 roots than in the large lesions in GN roots. In vitro bioassays revealed the $IC_{50}$ concentrations of anigorufone (**1**) necessary to immobilize and kill *R. similis*. These critical concentrations of active phenylphenalenones are not reached in the lesions of GN roots. In the sensitive GN cultivars, nematodes are neither immobilized nor killed and continue feeding and invading more tissue, creating larger lesions. In contrast, these critical concentrations are reached in Ykm5 roots and lead to the immobilization and eventual death of *R. similis* in situ. Hence, it appears that the biosynthesis of high concentrations of phenylphenalenones in the nematode-infected tissues in the roots of Ykm5 is the key mechanism responsible for Ykm5's resistance to *R. similis*. Phenylphenalenones do not create a nematode-toxic environment when they are present in roots at low concentrations. The local increase in concentration of these specialized metabolites upon nematode attack in resistant Ykm5 roots causes reduced motility and mortality, preventing nematodes from migrating to neighboring regions outside the initial infection zone.

To the best of our knowledge, the present bioassay-based study provides evidence of antinematode properties of phenylphenalenones and related compounds. Although bioassays were presumably performed with the active ingredients of both currently available and obsolete nematicides, and may have proved to be nematicidal in these tests, this information is not

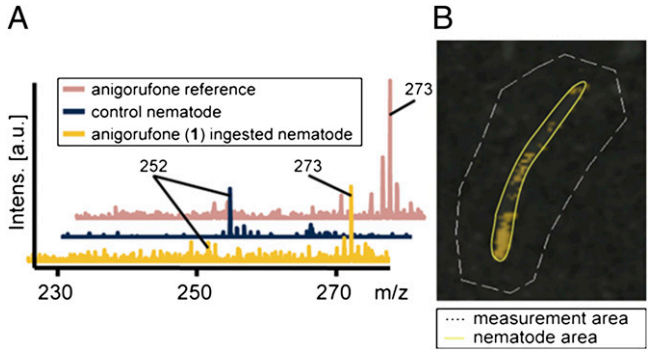


**Fig. 4.** Positive ion mode LDI-MSI of *R. similis* after motility bioassay with anigorufone (**1**). (*A*) Mass spectra in the range of *m/z* 185–285 from an imaging run of a nematode that had ingested anigorufone (**1**) and a control nematode in comparison with a mass spectrum of the anigorufone reference compound (**1**). (*B*) Image of a dried *R. similis* nematode before LDI-MSI overlaid with the image for the signal of *m/z* 273 $[M+H]^+$, representing anigorufone (**1**).

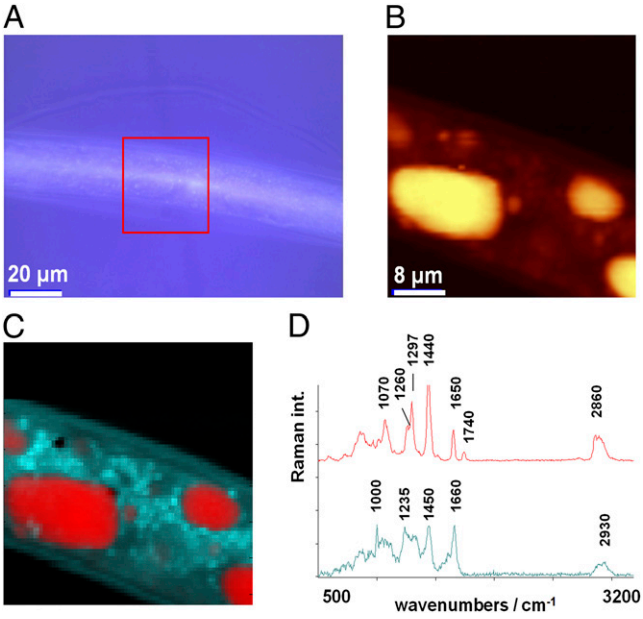


**Fig. 5.** BF picture of a nematode: (*A*) in comparison with a Raman image generated from the integrated Raman scattering intensities of C-H stretching vibrations (*B*). The plotted associated spectral information (*C*) and an image (*D*) was generated by plotting the abundances of the spectra associated with lipids (red) vs. proteins (light blue).

available to us in literature, as tests were part of company internal research and development work. Therefore, direct comparisons of anigorufone with nematicides, such as Nemacur, Temik, and Furadan are not feasible. Ferulic acid, a biosynthetic phenylpropanoid precursor of some phenylphenalenones (27), was recently shown to have nematostatic and nematocidal effects on *R. similis* (28). An $IC_{50}$ of 57, 84, and 42 $\mu g/mL^{-1}$ was obtained after 24-, 48-, and 72-h treatment, respectively. In comparison with ferulic acid, the $IC_{50}$ of anigorufone at 72 h was only 23 $\mu g/mL^{-1}$, showing that the latter is the stronger in planta antinematode compound. In addition, ferulic acid was not detected in the nematode induced lesions of our studied *Musa* cultivars. The most abundant compound, anigorufone (**1**), also proved to be the most active antinematode compound in the in vitro bioassays. Of the compounds tested, anigorufone (**1**) caused the greatest nematostatic and nematocidal effects. In addition to anigorufone (**1**), the compounds **2**, **4**, **8**, **11**, and **13** also had substantial nematostatic effects on *R. similis*, whereas others had less (compounds **5**, **9**, **10**, **12**, **15**) or no effect at all (compounds **6**, **14**). Whether or not the composition of the phytoalexin mixture present in lesions also contributes to the resistance seen in Ykm5 remains to be investigated. Testing selected combinations of different phenylphenalenones and whole extracts could reveal synergistic or antagonistic effects of individual phenylphenalenones (7).

The uptake of a plant secondary metabolite, anigorufone (**1**) by individual nematodes, was detected by LDI-MSI. No extraction of nematodes was necessary to analyze the ingested metabolites. Whether phenylphenalenones were incorporated into the nematode with the diet, via the skin, or via both routes was not addressed in this study. However, once taken up, nonglucosidic, poorly water-soluble phenylphenalenones, such as anigorufone (**1**), may converge with lipids. In this context, it was a remarkable finding that Raman microspectroscopy confirmed lipids as the major contents of yellow droplets in *R. similis*. In *Caenorhabditis elegans*, intestinal oil droplets—storage components for lipophilic compounds—are involved in minimizing the toxicity of polychlorinated biphenyl (29). A similar process may be indicated in *R. similis* by the observed formation of bulky oil droplets containing anigorufone (**1**). However, the enlargement of the oil droplets is not accompanied by an expansion of the nematode body limiting the space available to the internal organs and essential life processes. As opposed to the observed retention of lipids and the formation of bulky droplets in *R. similis*, a variety of stressors increased the excretion and stopped the pharyngeal pumping as a response in *C. elegans*. In this organism, a complex system of regulatory mechanisms can minimize the toxic effects of alcohol or heavy metals, at least for a limited time (30). Exposure of *C. elegans* to quercetin and caffeic acid resulted in an altered lipid metabolism with a reduced intestinal fat deposition. In contrast to the toxic effect of phenylphenalenones on *R. similis*, the tested compounds quercetin and caffeic acid caused an effect which is linked to longevity in *C. elegans* (31). Genes involved in regulation of lipid storage and mobilization (e.g., enlarged fat droplets in *C. elegans*) have been reported (32). Thus, the formation of large lipid droplets in *R. similis* upon exposure to phenylphenalenones may be an effect of these plant metabolites on the lipid regulatory system. The development of such bulky lipid droplets as part of the *Musa*–*R. similis* interaction may be comparable to the role of lipids in the aging of *C. elegans* (33).

Extrapolating data from laboratory bioassays to the field situation should be done with caution (34). Nevertheless, phenylphenalenones, both natural phytoalexins and synthetics, are potential pest control agents. However, regardless of their origin from plants or from chemical synthesis, phenylphenalenones as polycyclic aromatic compounds hold potential risks for farmers, consumers, nontarget organisms, and the environment. Adverse effects, such as phototoxicity of phenylphenalenone-producing plants and pure phenylphenalenones have been reported (35, 36). Hence, further investigations and risk assessments are necessary before considering phenylphenalenones as model compounds for the development of nematicides (7).

Metabolic engineering (37) to enhance the cellular concentration of inducible phenylphenalenones (phytoalexins) could be an appealing way to develop commercially important banana cultivars that are as resistant to *R. similis* as Ykm5 and as productive as GN is. Engineering of specialized metabolite pathways for enhancing the disease resistance represents a feasible strategy (38), but requires the genes and enzymes of the pathway and its regulation to be fully known. So far this is not the case for phenylphenalenone biosynthesis and, as a consequence, such studies are a necessary prerequisite. Moreover, the identification of the genes involved in local response to nematode attack and local induction of phenylphenalenone biosynthesis, as seen in Ykm5 and resulting in concentrations sufficient to control nematodes (or other pests), is challenging. The recent description of the draft sequence of the 523-megabase genome of a *Musa acuminata* doubled-haploid genotype represents a major advance to elucidate the complex biochemical processes of banana–pathogen interactions (39).

## Materials and Methods

Detailed experimental procedures are provided in *SI Material and Methods*. Briefly, the *Musa* cultivars were inoculated with a population of *R. similis*. The isolation, purification and structural elucidation of phenylphenalenones from lesions of root tissues were achieved by partition chromatography, semipreparative reversed-phase HPLC, and $^1$H NMR spectroscopy. LDI-MSI on the Ultraflex III and ultrafleXtreme mass spectrometers were used to localize phenylphenalenones in the lesions and anigorufone (**1**) in *R. similis*, respectively. Two series of in vitro bioassay experiments determined the effect of 13 phenylphenalenone-type compounds and the dosage effect of anigorufone (**1**) on the motility of the nematodes. Raman data of the lipid droplets were acquired with a confocal Raman microscope.

**ACKNOWLEDGMENTS.** We thank Lut Ooms, Tamara Krügel, and the greenhouse teams at the University of Leuven and the Max Planck Institute for Chemical Ecology for the help in raising *Musa* plants, and

Alexandra zum Felde for editorial help in the preparation of the manuscript. This study was supported in part by German Research Foundation [Deutsche Forschungsgemeinschaft (DFG)] Grants HO 4380/1 and SCHN 450/10 (to D.H. and B.S.); an Interfaculty Council for Development Cooperation, University of Leuven PhD scholarship (to S.D.); a grant by coopération européenne dans le domaine de la recherche scientifique et technique action 872 for a short-term scientific mission to the Max Planck Institute for Chemical Ecology (S.D.); a grant from the European Union 7th Framework Programme (Grant 305259) (to T.A.); the Dutch Polymer Institute (technology area high-throughput experimentation) (U.S.S.); Thüringer Ministerium für Bildung, Wissenschaft, und Kultur Grant B515-07008 (to U.S.S.); and the DFG (U.S.S.).

1. FAOSTAT (2011) Production (Crops) quantities of banana and plantains for 2011. *Food and Agriculture Organization of United Nations*. Available at faostat3.fao-org/faostat-gateway/go/to/download/Q/QC/E. Accessed October 15, 2013.
2. FAOSTAT (2011) Trade (Crops and livestock products) quantities of banana and plantains for 2011. *Food and Agriculture Organization of United Nations*. Available at faostat3.fao-org/faostat-gateway/go/to/download/T/TP/E. Accessed October 15, 2013.
3. Sarah JL (1999) *Diseases of Banana, Abacá and Ensete*, ed Jones DR (CABI Publishing, Wallingford, United Kingdom), pp 295–303.
4. Moens M, Perry RN (2009) Migratory plant endoparasitic nematodes: A group rich in contrasts and divergence. *Annu Rev Phytopathol* 47:313–332.
5. Campos VP, Villain L (2005) *Plant Parasitic Nematodes in Subtropical and Tropical* Agriculture, eds Luc M, Sikora RA, Bridge J (CABI Publishing, Wallingford, United Kingdom), 2nd Ed, pp 529–579.
6. Leach R (1958) Blackhead toppling disease of bananas. *Nature* 181(4603):204–205.
7. Chitwood DJ (2002) Phytochemical based strategies for nematode control. *Annu Rev Phytopathol* 40:221–249.
8. Quénéhervé P, Valette C, Topart P, Tezenas du Montcel H, Salmon F (2009) Nematode resistance in bananas: Screening results on some wild and cultivated accessions of *Musa* spp. *Euphytica* 165(1):123–126.
9. Wesseling C, et al. (2010) Symptoms of psychological distress and suicidal ideation among banana workers with a history of poisoning by organophosphate or N-methyl carbamate pesticides. *Occup Environ Med* 67(11):778–784.
10. zum Felde A, et al. (2009) The nematode burrowing of banana: Strategies for controlling the uncontrollable. *Acta Hortic* 828:101–108.
11. Grunewald W, Cannoot B, Friml J, Gheysen G (2009) Parasitic nematodes modulate PIN-mediated auxin transport to facilitate infection. *PLoS Pathog* 5(1):e1000266.
12. Dochez C, Whyte M, Tenkouano A, Ortiz R, De Waele D (2005) Response of east African highland bananas and hybrids to *Radopholus similis*. *Nematology* 7(5): 655–666.
13. Valette C, Andary C, Geiger JP, Sarah JL, Nicole M (1998) Histochemical and cytochemical investigations of phenols in roots of banana infected by the burrowing nematode *Radopholus similis*. *Phytopathology* 88(11):1141–1148.
14. Beckman CH (2000) Phenolic-storing cells: Keys to programmed cell death and periderm formation in wilt disease resistance and in general defence responses in plants? *Physiol Mol Plant Pathol* 57(3):101–110.
15. Wuyts N, et al. (2007) Potential physical and chemical barriers to infection by the burrowing nematode *Radopholus similis* in roots of susceptible and resistant banana (*Musa* spp.). *Plant Pathol* 56(5):878–890.
16. Collingborn FMB, Gowen SR, Mueller-Harvey I (2000) Investigations into the biochemical basis for nematode resistance in roots of three *musa* cultivars in response to *Radopholus similis* infection. *J Agric Food Chem* 48(11):5297–5301.
17. Cooke RG, Edwards JM (1981) Naturally occurring phenalenones and related compounds. *Fortschr Chem Org Naturst* 40:153–190.
18. Luis JG, Fletcher WQ, Echeverri F, Grillo TA (1994) Phenalenone-type phytoalexins from *Musa acuminata*—Synthesis of 4-phenyl-phenalenones. *Tetrahedron* 50(37): 10963–10970.
19. Wuyts N, De Waele D, Swennen R (2006) Activity of phenylalanine ammonia-lyase, peroxidase and polyphenol oxidase in roots of banana (*Musa acuminata* AAA, cvs Grande Naine and Yangambi km5) before and after infection with *Radopholus similis*. *Nematology* 8(2):201–209.
20. Winters K, Batterton JC, Van Baalen C (1977) Phenalen-1-one: Occurrence in a fuel oil and toxicology to microalgae. *Environ Sci Technol* 11(3):270–272.
21. Otálvaro F, et al. (2007) Phenalenone-type compounds from *Musa acuminata* var. "Yangambi km 5" (AAA) and their activity against *Mycosphaerella fijiensis*. *J Nat Prod* 70(5):887–890.
22. Jitsaeng K, Schneider B (2010) Metabolic profiling of *Musa acuminata* with *Sporobolomyces salmonicolor*. *Phytochem Lett* 3(2):84–87.
23. Hirai N, Ishida H, Koshimizu K (1994) A phenalenone-type phytoalexin from *Musa acuminata*. *Phytochemistry* 37(2):383–385.
24. Hölscher D, et al. (2009) Matrix-free UV-laser desorption/ionization (LDI) mass spectrometric imaging at the single-cell level: Distribution of secondary metabolites of *Arabidopsis thaliana* and *Hypericum* species. *Plant J* 60(5):907–918.
25. Alexandrov T, et al. (2010) Spatial segmentation of imaging mass spectrometry data with edge-preserving image denoising and clustering. *J Proteome Res* 9(12):6535–6546.
26. Klapper M, et al. (2011) Fluorescence-based fixative and vital staining of lipid droplets in *Caenorhabditis elegans* reveal fat stores using microscopy and flow cytometry approaches. *J Lipid Res* 52(6):1281–1293.
27. Schmitt B, Hölscher D, Schneider B (2000) Variability of phenylpropanoid precursors in the biosynthesis of phenylphenalenones in *Anigozanthos preissii*. *Phytochemistry* 53(3):331–337.
28. Wuyts N, de Waele D, Swennen R (2006) Effects of plant phenylpropanoid pathway products and selected terpenoids and alkaloids on the behavior of the plant-parasitic nematodes *Radopholus similis*, *Pratylenchus penetrans* and *Meloidogyne incognita*. *Nematology* 8(1):89–101.
29. Menzel R, et al. (2007) Cytochrome P450s and short-chain dehydrogenases mediate the toxicogenomic response of PCB52 in the nematode *Caenorhabditis elegans*. *J Mol Biol* 370(1):1–13.
30. Jones D, Candido EPM (1999) Feeding is inhibited by sublethal concentrations of toxicants and by heat stress in the nematode *Caenorhabditis elegans*: Relationship to the cellular stress resonance. *J Exp Zoolog A Comp Exp Biol* 284(2):147–157.
31. Pietsch K, et al. (2011) Hormetins, antioxidants and prooxidants: Defining quercetin-, caffeic acid- and rosmarinic acid-mediated life extension in *C. elegans*. *Biogerontology* 12(4):329–347.
32. Ashrafi K, et al. (2003) Genome-wide RNAi analysis of *Caenorhabditis elegans* fat regulatory genes. *Nature* 421(6920):268–272.
33. Hou NS, Taubert S (2012) Function and regulation of lipid biology in *Caenorhabditis elegans* aging. *Front Physiol* 3:143.
34. Spence KO, Lewis EE, Perry RN (2008) Host-finding and invasion by entomopathogenic and plant-parasitic nematodes: Evaluating the ability of laboratory bioassays to predict field results. *J Nematol* 40(2):93–98.
35. Darwin C (1866) *On the Origin of Species by Means of Natural Selection* (John Murray, London), 4th British Ed, p 12. Available at darwin-online.org.uk/Variorum/1866/1866-12-dns.html. Accessed November 25, 2013.
36. Flors C, et al. (2006) Phototoxic phytoalexins. Processes that compete with the photosensitized production of singlet oxygen by 9-phenylphenalenones. *Photochem Photobiol* 82(1):95–103.
37. Misawa N (2011) Pathway engineering for functional isoprenoids. *Curr Opin Biotechnol* 22(5):627–633.
38. Collinge DB, Jørgensen HJL, Lund OS, Lyngkjaer MF (2010) Engineering pathogen resistance in crop plants: Current trends and future prospects. *Annu Rev Phytopathol* 48:269–291.
39. D'Hont A, et al. (2012) The banana (*Musa acuminata*) genome and the evolution of monocotyledonous plants. *Nature* 488(7410):213–217.